Heterogeneous crystal nucleation on bubbles in silicate melt

MARK J. DAVIS* AND PHILLIP D. IHINGER

Department of Geology and Geophysics, Yale University, 210 Whitney Avenue, New Haven, Connecticut 06511, U.S.A.

ABSTRACT

Experiments reported herein document heterogeneous crystal nucleation on bubbles in supercooled lithium disilicate melt. Crystalline lithium disilicate ($Li_2Si_2O_5$) nucleated and grew on small bubbles (~1 μm) with a one-to-one correspondence between the number of bubbles and crystals (ranging from <10^2 to ~10^5 bubbles/mm³). Crystals grew on large bubbles (>100 μm) only in samples fused in N_2, suggesting a chemical control on nucleating efficiency. Bubbles ~1 μm in diameter served as nucleation sites for polycrystalline lithium disilicate spherulites; bubbles smaller than ~1 μm served as nucleation sites for the more common ellipsoidal crystalline form. This difference in behavior might be due to the additional surface area available for crystal nucleation on the 1 μm bubbles.

Our findings suggest that superliquidus thermal history can influence crystal nucleation via bubble formation induced by supersaturation, and has implications for both natural samples and experimental studies. Heterogeneous crystal nucleation on bubbles may serve as an efficient nucleation mechanism in natural degassing magmas and may aid in the formation of fine-grained groundmasses common to many volcanic rocks. Furthermore, we have documented a new mechanism of spherulite formation in highly supercooled silicate melt, similar to conditions thought to exist during devitrification of natural glasses. The ability of crystals to nucleate on bubbles can be exploited in the production of commercial glass-ceramic materials.

INTRODUCTION

Nucleation kinetics play a central role in the development of crystalline texture in igneous and metamorphic rocks, and in commercial glasses and glass-ceramic materials. Nucleation can occur on pre-existing surfaces (heterogeneous: Berkebile and Dowty 1982; Holand et al. 1995) or in the absence of such surfaces (homogeneous: James 1974; Christian 1975). The effects of added impurities (Schlesinger and Lynch 1989; Narayan et al. 1996), water content (Gonzalez-Oliver et al. 1979; Davis et al. 1997), and thermal history (Lofgren 1983; Baker and Grove 1985; Mishima et al. 1996; Davis 1996) on both homogeneous and heterogeneous crystal nucleation in silicate melts have been investigated. In addition, the role of crystal surfaces on bubble nucleation has been analyzed (e.g., Wilcox and Kuo 1973; Hurwitz and Navon 1994). Here we report experimental results that document crystal nucleation on vapor bubbles in silicate melt. Crystal nucleation on bubbles has been observed only rarely. One notable example is Schmelzer et al. (1993), who reported crystallization on bubbles in $NaPO_3$ melt. To our knowledge, crystal nucleation on bubbles has not been reported for silicate melts, either natural or synthetic. We believe the possible consequences of crystal nucleation on bubbles to erupting natural magmas are significant enough to warrant further investigation.

Previous studies of nucleation kinetics in lithium disilicate ($Li_2Si_2O_5$) melts have noted the presence of two populations of crystals in experimental charges: (1) the common ellipsoidal form of stoichiometric lithium disilicate; and (2) spherulites of the same material (e.g., James 1974; Davis 1996). The first morphology, the more common of the two in crystal nucleation experiments (e.g., Matusita and Tashiro 1973; James 1974; Davis et al. 1997), has been attributed to a homogeneous nucleation mechanism. During a systematic study of the influence of water on nucleation kinetics in silicate melt (Davis et al. 1997), we observed that a preliminary sample preparation method resulted in the (reproducible) development of a very high number density (~10^4 crystals/mm³) of spherulites. This sample preparation method consisted of re-fusing glass cubes at a lower temperature than the initial fusion temperature of the starting material (1120 vs. 1350 °C). Upon closer inspection of the spherulites, it was discovered that every spherulite contained a ~1 μm bubble at its center. In contrast, when we re-fused our samples at a temperature equal to that of the initial fusion, no spherulites were observed in our quenched samples. The latter sample preparation method was used for the experiments reported in Davis et al. (1997) to ensure that only homogeneous crystal nucleation occurred. We consider in this report the nucleation of crystals on bubbles. As discussed below, the presence of crystals serves to "tag" very small bubbles that might otherwise have gone un-

---

noticed. In addition, crystal morphology and the observed efficiency with which certain bubbles served as nucleation sites provide insight into heterogeneous crystal nucleation kinetics.

EXPERIMENTAL METHODS

Several sets of experiments were designed to investigate the influence of bubble size and bubble composition on crystal nucleation efficiency (heterogeneous site "activity") and crystal morphology. The experimental method sample preparation and analysis procedures are described more fully in our companion paper that investigates bubble nucleation (Davis and Ihinger 1998, unpublished data). Briefly, homogeneous 25 g slugs of lithium disilicate glass were formed through fusion of well-mixed reagent-grade lithium carbonate and silica powders at 1350 °C in a Deltech gas-mixing furnace using dry air, N_2, or Ar. Sample cubes (~2 mm) were cut from each slug and re-fused to form round beads in a variety of gas mixtures, including: (1) dry N_2 (<1 ppm H_2O); (2) purified dry air; (3) purified air with controlled amounts of water vapor using an apparatus described in Davis (1994); (4) CO_2; (5) Ar; (6) He (the latter three gases with <50 ppb H_2O); and (7) ambient air. Re-fusion conditions (temperatures and durations) were varied in an attempt to induce bubble formation. Nearly all experiments concluded with a 6 min heat treatment at 600 °C in air to nucleate and grow crystals heterogeneously on bubbles and to grow the crystals to observable size; during this heat treatment no new bubbles formed, nor was there any significant homogeneous crystal nucleation. Scanning electron microscopy (SEM) was conducted using a JEOL 8600 instrument operated at 10 kV accelerating voltage and ~30 pA current. Samples for SEM imaging were etched lightly in HF prior to carbon coating.

RESULTS

The great abundance of the atypical spherulitic form of lithium disilicate in preliminary experiments was the first indication of a previously unrecognized phenomenon (Davis and Ihinger 1998, unpublished data). Figure 1a shows a typical experimental charge that exhibits two spatially distinct populations of crystals: (1) crystals homogeneously distributed throughout the interior of the sample (Fig. 1b); and (2) heterogeneously distributed crystals aligned in sub-linear chains emanating from the sample rim (Fig. 1c). Essentially every ~1 μm bubble observed in every experiment was surrounded by crystalline lithium disilicate in spherulitic form. Furthermore, every spherulite in experiments of 30 min duration contained a ~1 μm bubble at its core. Taken together, these observations indicate a one-to-one correspondence between the number of ~1 μm bubbles and spherulites in 30 min experiments (Table 1, cf. L25-381, 382). Longer duration re-fusions resulted in similar spatial distributions of crystals; however, both the ratio of spherulitic to ellipsoidal crystal forms and total crystal number densities decreased with increasing re-fusion duration (Davis and
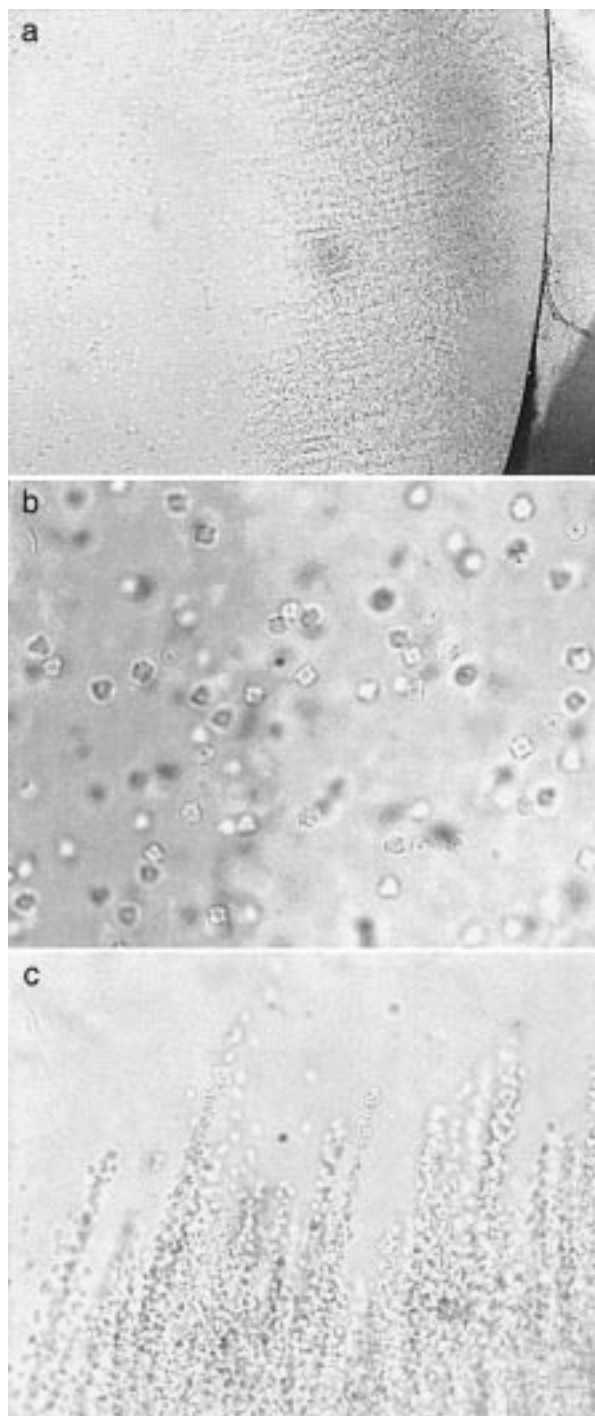

FIGURE 1. (a) Photomicrograph of "interior" and "rim" population of bubbles (air cube re-fused at 1120 °C for 2 min in ambient air). Sharp line at right is sample border (width of photo is 0.75 mm). (b) Interior bubble population, containing numerous ~10 μm spherulites (air cube re-fused at 1120 °C for 30 min in ambient air). (c) Stringer population of bubbles along sample rim (N_2-cube re-fused at 1120 °C for 30 min in ambient air). Width of (b) and (c) photos is 0.3 mm. All crystals in all three photos contain a ~1 μm bubble; only those in the plane of focus are discernible and appear as small black dots. All experiments in Figure 1 included a 6 min heat treatment at 600 °C.
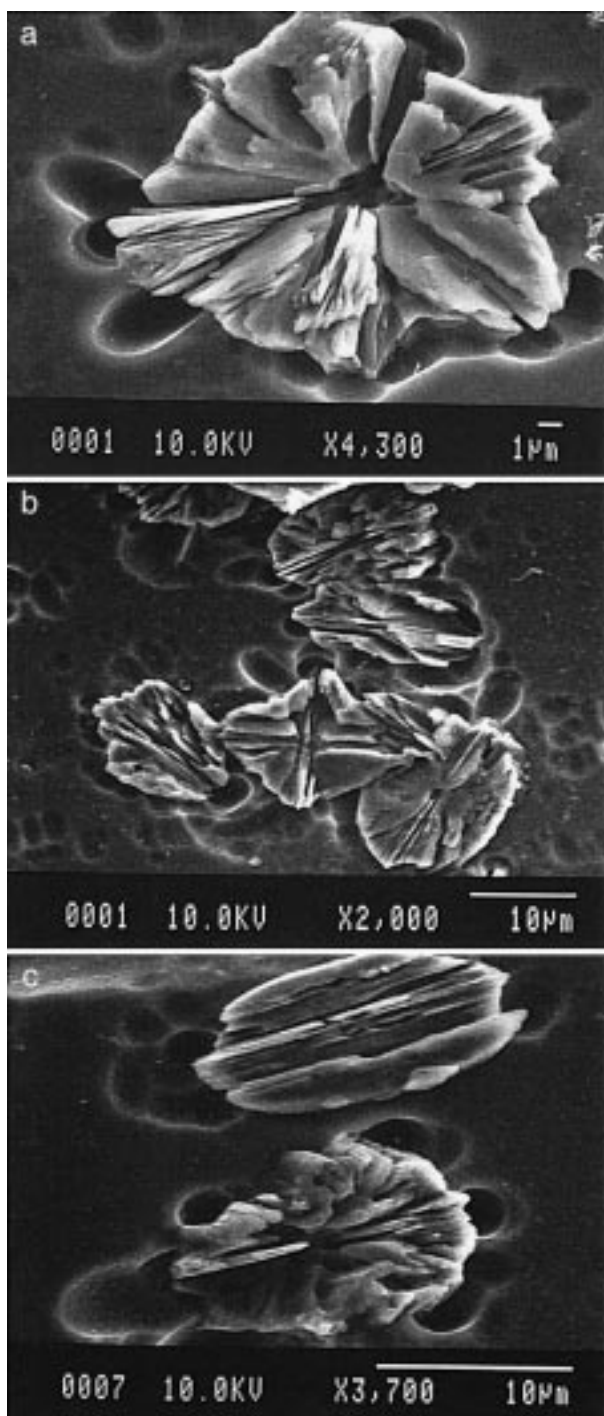
FIGURE 2. SEM images of various crystalline morphologies. All samples were etched in concentrated HF for ~5 s to delineate features. Localized and isolated dissolution of glass immediately surrounding crystals was the result of the acid etch. (**a**) SEM image of a small spherulite. At least four domains are apparent, each defined by parallel crystalline sheets; each domain is separated by planes along which sheets are truncated. Inner cavity marks location of bubble. (**b**) and (**c**) Variety of crystals with ellipsoidal forms, each displaying constrained branching, in which all sheets are parallel to a common line, in contrast to (**a**);

Ihinger 1998, unpublished data). This change coincided with a progressive decrease in bubble size to the point where few bubbles could be observed with optical microscopy. Abundant ellipsoidal crystals remained, however, with a spatial distribution still corresponding roughly to that shown in Figure 1a.

Interior bubbles with associated spherulites were most abundant in experiments that involved a second fusion at 1120 °C (L2S-312, 324, 335-6, 381-2, 407, 419, and 459) or in samples fused in Ar (L2S-393-4, 439, 452, 457, 458-9). Fewer bubbles formed in high water content samples (L2S-373, 404-5). Experiments that involved two high-temperature re-fusions (1350 followed by 1120 °C) produced numerous interior bubbles only if Ar was used. Davis and Ihinger (1998, unpublished data) concluded that Ar was the dominant gas species responsible for interior bubble formation in experiments that used air- and N_2-cubes. Thus, bubble interfaces were probably in equilibrium with an Ar-rich atmosphere. Rim bubbles formed during crystallization initiated on the sample exterior during heating from room temperature to fusion conditions.

Nearly all charges contained at least a few large bubbles (~100 μm). Large bubbles from cubes fused under either Ar, air, or air-water gas mixtures did not serve as crystal nucleation sites. Large bubbles from cubes fused under N_2, however, did serve as crystal nucleation sites; numerous spherulites (see below) surrounded each large bubble. This suggests that the gas species present, either dissolved in the melt or that which fills the bubbles, influences heterogeneous crystal nucleation on bubbles.

SEM imaging revealed a considerable amount of detail concerning crystalline morphologies. Two principal varieties of crystal forms exist: spherulites (Fig. 2a) and ellipsoidal forms (Figs. 2b and 2c). Sheet-like structures are evident in both types of morphologies, consistent with the sheet silicate form of crystalline lithium disilicate. Both spherulitic and ellipsoidal forms (Fig. 2a) exhibit branching from a central ~1 μm bubble. Branching is manifested by the presence of at least four domains, each of which is defined by parallel sheets. Domain boundaries are delineated by angular discordance with adjacent domains. The only obvious difference between ellipsoidal and spherulitic morphologies is that all sheets are parallel to a common axis in ellipsoidal forms whereas this constraint is not observed in spherulitic forms. We argue below that this difference arises from variations in crystal nucleation densities.

We subjected certain charges to extended growth treatments to obtain improved imaging of crystal morphology. In so doing, we discovered that the common spherulitic form is apparently not stable at larger crystal sizes. Con-

←

note well-defined location of bubble in bottom right crystal in (**b**). (**a**) through (**c**) are from same sample charge (air cube refused at 1120 °C for 30 min in ambient air followed by a 6 min heat treatment at 600 °C).
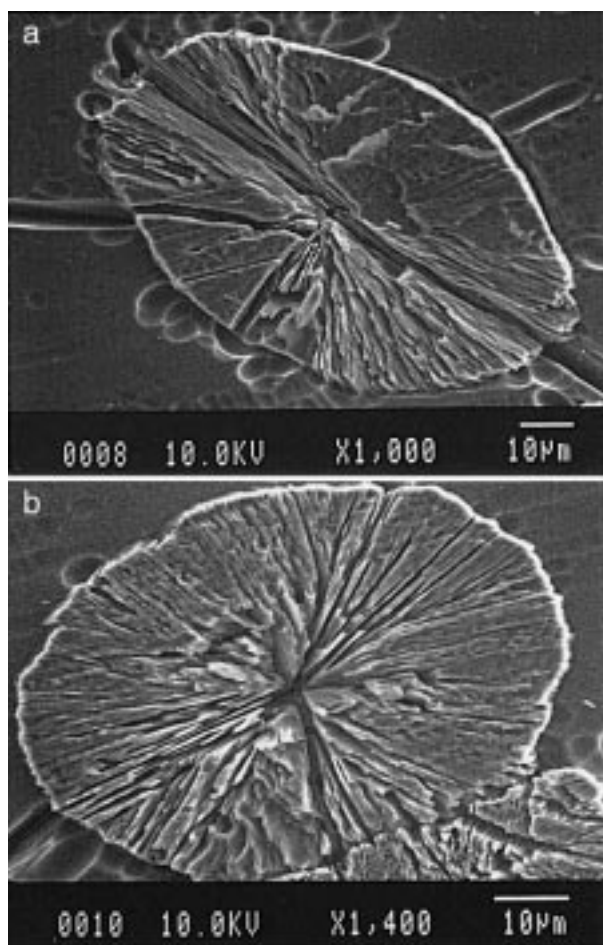
FIGURE 3. (**a**) SEM image of large ellipsoidal crystal observed with long axis roughly parallel to plane of photo. (**b**) SEM image of large ellipsoidal crystal with long axis perpendicular to photo. Note similar branching style as in Figures 2b and 2c for small ellipsoids. Both photos are from same sample (air cube refused at 1120 °C for 2 min then heated at 600 °C for 30 min)

tinued growth of small spherulitic crystals resulted in a change to the ellipsoidal form. The experiment depicted in Figure 3 was designed to produce small spherulites following a 6 min heat treatment (as in Fig. 1b) but instead was subjected to a 30 min heat treatment, thereby growing the crystals to ~30 μm size. All crystals in this sample are ellipsoidal. Figures 3a and 3b show two orientations of lithium disilicate crystals, one oriented roughly along the major axis of the ellipse (Fig. 3a) and the other perpendicular to the major axis. The first orientation reveals that sheets in these large crystals are all sub-parallel to a line that defines the long axis, similar to that observed in small ellipsoidal crystals (Fig. 2b). The view perpendicular to the long axis (Fig. 3b) reveals that there are at least six discrete domains within which adjacent sheets are parallel; adjacent domains are discordant. These images are similar to those obtained by James

and Keown (1974) using TEM on 10–100 μm lithium disilicate crystals nucleated and grown at 560 °C.

Standard thin sections (~30 μm thick) were made of representative experimental charges to examine crystal morphologies. The spherulites in this study consist of polycrystalline aggregates, typically from four to six crystals per bubble. The term "polycrystalline" is used to denote a lack of any obvious crystallographic relationship between adjacent domains (Fig. 2a), in contrast to the ellipsoidal forms that contain a common line of symmetry (Figs. 2b, 2c, and 3). Each spherulite exhibited an extinction cross regardless of orientation, a characteristic feature of spherulites that is attributed to fine, radiating crystalline lamellae inherent to spherulite structure (Khoury and Passaglia 1976). In contrast, ellipsoidal forms, when viewed with their long axis in the plane of the thin section, underwent extinction as a coherent, single unit. However, when viewed with their long axis perpendicular to the plane of the thin section, ellipsoidal forms underwent progressive extinction as the stage was rotated, similar to the spherulites. This suggests that the ellipsoidal forms do not contain only one crystallographic orientation, consistent with our SEM imaging (Fig. 2b).

DISCUSSION

Crystal nucleation kinetics

Our results document the efficiency with which bubbles can serve as nucleation sites for crystals. We observed a one-to-one correspondence between the number of small bubbles and crystals. Given the propensity of many silicate compositions to crystallize on external surfaces, including those that do not nucleate homogeneously, such as sodium disilicate (Matusita and Tashiro 1973), cristobalite (Fratello et al. 1980), and plagioclase (Kirkpatrick et al. 1979), it is somewhat surprising that crystal nucleation on bubbles is not observed more commonly. This may be due to the difficulty of observing micron to sub-micron bubbles by optical means, although this difficulty is partially circumvented using electron imaging techniques (e.g., Klug and Cashman 1994). We have shown that bubble surfaces can act as nucleation sites, but that the presence of a surface is not sufficient to guarantee crystal nucleation, as indicated by large (~100 μm) crystal-free bubbles (e.g., this study; Hurwitz and Navon 1994; Bagdassarov et al. 1996).

Our results serve to demonstrate that bubble surfaces exhibit crystallization behavior distinct from planar sample exterior surfaces. Crystallization was observed on all exterior sample surfaces with an approximate crystal number density of 10^3 crystals/mm². Although all small bubbles acted as crystal nucleation sites in this study, only some of the large bubbles served as crystal nucleation sites. The differences in nucleating effectiveness for different types of bubbles observed in this study indicate a control on heterogeneous crystal nucleation beyond the mere presence of an interface. Lithium disilicate crystals nucleated on small bubbles (all samples) and on large

TABLE 1. Experimental results

Sample no.	Starting mat.*	Re-fusion cond.‡				Bubbles (mm⁻³)	Comments†
		Gas	pH₂O	T	t		
L2S-312	MD-10	N₂	0	1120	30	1.17×10^3	drop quench
L2S-324	MD-12	Air	0	1120	30	5.83×10^4	drop quench
L2S-335	MD-12	Air	0	1120	30	6.51×10^4	
L2S-336	MD-12	Air	171	1120	30	1.02×10^5	similar to L2S-335, but with larger crystals due to higher [H₂O] in furnace
L2S-373	MD-13	Air	355	1350	30	6.00×10^1	
L2S-381	MD-13	Air	0	1120	30	3.20×10^3	no growth treatment; cf. L2S-382
L2S-382	MD-13	Air	0	1120	30	3.48×10^3	cf. L2S-381; considerable healing of rim even with dry air re-fusion
L2S-393	MD-11	Ar	0	1350	30	7.98×10^4	2-stage re-fusion: 30 min at 1120 °C in Ar; core region: 2.79 × 10² bubble number density
L2S-394	MD-11	Ar	0	1350	30	1.48×10^2	rim number density = 1.33 × 10⁴
L2S-404	MD-13	Air	760	1350	30	9.43×10^2	2-stage re-fusion: 5 min at 1120 °C in Lindberg; bubbles inhomogeneously distributed
L2S-405	MD-13	Air	760	1350	30	3.36×10^2	cf. L2S-404; through-going stringers throughout charge
L2S-407	MD-13	Air	0	1120	30	3.44×10^3	cf. L2S-406, 459
L2S-419	MD-13	Air	43	1120	30	1.27×10^2	Lindberg
L2S-438	MD-11					6.38×10^2	cube; no rim
L2S-439	MD-11	Ar	0	1350	120	9.67×10^3	
L2S-451	MD-13	Ar	0	1350	120	1.19×10^3	inhomogeneous bubble streamers across charge
L2S-452	MD-10	Ar		1350	120	6.46×10^2	inhomogeneous bubble streamers across charge
L2S-453	MD-11	Air	0	1350	30	2.38×10^1	no rim
L2S-454	MD-11	Air	0	1350	120	1.58×10^1	no rim
L2S-455	MD-11					4.94×10^2	cube; cf. L2S-438; no rim
L2S-456	MD-11	Air	14	1350	2	7.97×10^1	no rim
L2S-458	MD-11					7.86×10^2	cube; cf. L2S-438, 455; no rim
L2S-459	MD-12	Air	0	1120	30	4.51×10^4	cf. L2S-407

  * MD-10 = fused in dry N₂ at 1350 °C; MD-11 = fused in dry Ar at 1350 °C; MD-12 and MD-13 = fused in dry air at 1350 °C.
  † Except where noted, all samples were re-fused beads, quenched in air by extraction from Deltech furnace. Experiments conducted in vertical Lindberg furnace noted (pH₂O ~ 43 torr). Unless otherwise noted, all samples had a bubble-rich rim (~200 to 400 μm; see text).
  ‡ Re-fusion condition units: p_H₂O (torr); T (°C); t (min).

bubbles (~100 μm) in samples re-fused in an N₂ atmosphere, but not on large bubbles in samples re-fused in other atmospheres.

Previously, Leko and Komarova (1975) had examined the surface crystallization of quartz in fused silica (pure SiO₂) in atmospheres of variable composition. They noted that bubbles (size not reported) containing a variety of gas species (including O₂, H₂O, CO₂, H₂, CO, NO, and N₂) did not serve as nucleation sites. However, if these bubbles were exposed to the ambient atmosphere, the rate of crystallization on newly exposed bubble surfaces during thermal treatment was as fast as that observed on external surfaces not associated with exposed bubbles. Moreover, exposed bubble surfaces from samples fused under highly reducing conditions crystallized much earlier and faster than external surfaces not associated with exposed bubbles. Leko and Komarova (1975) concluded that surface chemical reactions play an important role for crystallization on exposed bubble surfaces. Our results concerning the effectiveness of large, possibly nitrogen-filled internal bubbles to serve as crystal nucleation sites corroborate this conclusion. Additional work will be necessary to characterize adequately the role of gas chemistry on crystal nucleation kinetics.

Insight into how surface chemistry can influence heterogeneous crystal nucleation can be gained through consideration of classical nucleation theory. A general equation for the rate of steady-state nucleation (I) in condensed systems has the following form (Christian 1975):

$$I = \frac{A}{\eta} \exp\left(\frac{-\Delta G^*}{kT}\right) \qquad (1)$$

where A represents a jump frequency and is relatively weakly temperature dependent, k is the Boltzmann constant, T is temperature (K), η is dynamic viscosity, and ΔG^* is the thermodynamic energy barrier to form a nucleus of the critical size, such that

$$\Delta G^* = \frac{16\pi\sigma^3 V_m^2}{3\Delta G_c^2} \qquad (2)$$

where σ is surface free energy, V_m is molar volume of the melt, and ΔG_c is the bulk free energy change for crystallization. Equation 2 describes homogeneous nucleation kinetics; the heterogeneous case only modifies the surface free energy term in Equation 2 (Christian 1975):

$$\sigma^3 = \sigma_\infty^3 f(\theta) \qquad (3)$$

where σ_∞ is the surface free energy between the crystal and liquid in the absence of a heterogeneity (surface), θ is the contact angle between crystal and heterogeneity, and

$$f(\theta) = (2 - 3\cos\theta + \cos^3\theta)/4 \qquad (4)$$

for a spherical cap model. Owing to the extreme dependence of the nucleation rate on the surface free energy, small changes in σ result in large changes in I. For example, a 30% decrease in σ results in a 10^9 increase in the nucleation rate using parameter values for lithium disilicate (Zanotto and James 1985). Bubble surfaces in aqueous solutions can maintain chemical compositions distinct from those of the bulk liquid or bubble constituents due to surface energy effects (Rosen 1989). The presence of a chemical heterogeneity at the bubble-liquid interface would be expected to lower the surface free energy via the formation of a surfactant layer (Rosen 1989). Furthermore, if the chemistry of the bubble-liquid interface was controlled by the gas species present in the bubble, the identity of the gas species could modify the nature and influence of a possible surfactant phase. We thus speculate that the nucleating effectiveness of large ($\sim$100 μm) bubbles was due to surface chemical effects, perhaps related to the formation of a surfactant at the bubble-liquid interface.

Effect of bubble size on crystal morphology

Our results document that bubble size influences crystal habit: $\sim$1 μm bubbles were surrounded by spherulites, whereas smaller bubbles were surrounded by the more common ellipsoidal habit. The fundamental difference between crystals nucleated on small ($<$1 μm) and somewhat larger ($\sim$1 μm) bubbles is thus whether an ellipsoidal form or a polycrystalline spherulite is the preferred morphology. This difference in behavior might simply be related to the available surface area on the bubble. The number density of crystals that nucleate and grow on the external interface of the sample after 6 min at 600 °C in air may be used as a comparison for the number that grow on an interior bubble surface at 600 °C. Note that crystals nucleated and grown on the sample exterior did so in an air atmosphere, whereas bubble interfaces were likely in equilibrium with an Ar-rich atmosphere (Davis and Ihinger 1998, unpublished data). The exterior surface number density ($\sim$10³/mm²) makes it unlikely that a 0.5 μm bubble, with a surface area of $\sim$3 $\times$ 10⁻⁶ mm², would be a nucleation site, although nucleation is observed in our experiments. Thus, the nucleation rate of crystals on bubbles is at least three orders of magnitude higher than that observed on the external interface and is likely due to the physical and chemical nature of the bubble surface. An average number density of crystals $\sim$10⁶/mm² on bubble surfaces would result in approximately one crystal per 0.5 μm bubble. As the bubble surface area depends on the square of the bubble radius, relatively small changes in bubble radius might have a large effect. For example, a bubble with 1 μm diameter and a surface area $\sim$10⁻⁵ mm² would be expected to nucleate $\sim$4 crystals. This prediction is in broad accord with the observed polycrystalline spherulites on 1 mm bubbles (e.g., Fig. 2a). Thus, it is possible that polycrystalline aggregates tend to form on large bubbles simply because of the larger surface area of such bubbles, which allowed for the nucleation of several crystals. Conversely, smaller bubbles favored fewer crystal nucleation events.

Implications to geology and glass science

Because the formation of bubbles is an inevitable consequence of volcanic eruptions, determining the influence, if any, of bubbles on the crystallization of a degassing magma is important to Earth scientists. The possible implications of a previously unrecognized crystallization process that involves ''armoring'' of newly formed bubbles by crystals require examination. Vesicles (bubbles) are thought to be responsible for the formation of amygdules and lithophysae during late-stage crystallization or subsequent low-temperature alteration of lavas. However, these features are related to crystallization from the fluid phase within bubbles; we describe crystallization from the melt on bubbles. Moreover, spherulites similar to those observed in our study are commonly found in natural glasses (e.g., Lofgren 1971). We have described a previously unrecognized process by which spherulites are formed in a melt system.

One possible consequence of crystals nucleating on bubbles in cooling, degassing magmas is the potential influence on rock texture. We have observed a one-to-one correspondence between the number of $\sim$1 μm bubbles and spherulites, indicating that bubble nucleation exerts a direct control over the final crystal number density in our experiments. It is expected that an ascending magma experiences volatile supersaturation and subsequent bubble nucleation at some critical depressurization (e.g., Taylor et al. 1983; Hurwitz and Navon 1994) and would be synchronous with crystallization, owing to both overall cooling and an increase in liquidus temperature due to devolatilization (Cashman et al. 1996). If crystals nucleated readily on small bubbles formed in such a process, a fine-grained, high-number density groundmass would likely result.

A groundmass consisting of plagioclase $\pm$ pyroxene is very common in volcanic rocks [$<$10⁵ to 10⁸ crystals/mm³ (e.g., Cashman and Marsh 1988; Cashman 1992), similar to bubble number densities reported here], which is normally attributed to rapid cooling at near-surface conditions. It is possible that groundmass formation is facilitated by the presence of small bubbles formed during the eruptive process. Such bubbles could be extremely small ($<<$1 μm) and still conceivably serve as crystal nucleation sites, thereby limiting their detection to nanometer-scale imaging techniques. Furthermore, the amount of gas necessary to produce small bubbles requires only ppm to sub-ppm concentrations in the melt, levels typically encountered for a wide variety of gas species (e.g., Carroll and Holloway 1994).

Relatively few studies have linked bubbles directly with crystal nucleation and growth. Balk and Krieger (1936) describe spherulites in devitrified felsite dikes that contain numerous liquid or gaseous inclusions. Given that

numerous bubbles are enclosed by each crystal, unlike the one-to-one correspondence between bubbles and crystals in this study, it is likely that these authors observed bubbles that formed as a consequence of crystallization. Bubbles were incorporated into crystals in much the same way rim bubbles were formed in our experiments. Boffé et al. (1962) observed numerous bubbles accompanying crystallization and re-melting of crystals in glass-ceramic materials. They interpreted bubble formation in their experiments as mostly due to volatile rejection from nominally anhydrous crystals, again similar to our rim bubbles. Philpotts and Lewis (1987) ascribe the formation of pipe vesicles in basaltic lava flows to the same mechanism. Planner (1979) observed a close association of olivine crystals with bubbles in his crystallization experiments involving chondritic melts. He interpreted the resulting textures as having arisen from heterogeneous nucleation of crystals on bubbles. However, inspection of Planner's photomicrographs reveals no clear spatial correlation between bubbles and crystals, with the exception of some olivine phenocrysts containing numerous small bubbles, again suggestive of volatile exsolution rather than crystal nucleation on bubbles.

Geologists have long sought a definitive explanation of spherulite formation in glassy volcanic rocks (e.g., Kesler and Weiblen 1968; Lofgren 1971; Maleev 1972). Ongoing questions include the time-temperature history necessary to induce devitrification of volcanic glasses and the role of external fluids in promoting crystallization. In some cases a dependence of spherulite formation on pre-existing heterogeneities is evident, including microlites and fractures (Lofgren 1971). We have documented a new mechanism of spherulite formation in highly supercooled silicate melt, similar to conditions thought to exist during devitrification of natural glasses.

Nucleation of crystals on bubbles in the lithium disilicate system suggests a new method to produce commercial glass-ceramic materials. For most melt compositions, impurities must be added to promote crystal nucleation (e.g., TiO_2; Doremus 1994). In contrast, bubble formation requires only the presence of a dissolved volatile constituent in excess of its solubility limit. In lithium disilicate, only Ar and H_2O served as a significant bubble-forming volatile species; different melt compositions might require other volatile components for efficient bubble formation. To make the process feasible, however, bubbles must not only be present, but they also must serve as crystal nucleation sites. We have demonstrated (Davis and Ihinger 1998, unpublished data) that bubble size and the identity of the gas species influences the nucleating effectiveness of bubbles and the resultant crystal habit. Controlling these two independent parameters might allow sufficient design control to make the process feasible for arbitrary melt compositions.

More work is needed to evaluate the role that bubbles play in crystallization of natural silicate melt. We have documented that crystals can nucleate on bubbles in the lithium disilicate system. This has immediate relevance to glass scientists, for whom the lithium disilicate system is of direct interest and the control of bubbles of great importance. Lithium disilicate has long served as the model system for nucleation studies of silicate compositions, and a thorough understanding of all crystallization mechanisms that operate in this system is required. We have shown that a previously unrecognized crystallization mechanism exists in this and possibly other melt systems and a re-evaluation of some earlier experimental and field studies may be required. An understanding of the competing effects of homogeneous vs. heterogeneous nucleation and the various modes of subsequent crystal growth are required to understand fully the solidification history of synthetic as well as natural systems. We have demonstrated that bubbles can take an active role in the crystallization process in silicate melt.

References cited

Bagdassarov, N.S., Dingwell, D.B., and Wilding, M.C. (1996) Rhyolite magma degassing: an experimental study of melt vesiculation. Bulletin of Volcanology, 57, 587–601.

Baker, M.B. and Grove, T.L. (1985) Kinetic controls on pyroxene nucleation and metastable liquid lines of descent in a basaltic andesite. American Mineralogist, 70, 279–287.

Balk, R. and Krieger, P. (1936) Devitrified felsite dikes from Ascutney Mountain, Vermont. American Mineralogist, 21, 516–522.

Berkebile, C.A. and Dowty, E. (1982) Nucleation in laboratory charges of basaltic composition. American Mineralogist, 67, 886–899.

Boffé, M., Pecriaux, G., and Plumat, E. (1962) Formation of bubbles during devitrification and remelting of crystals in glass. In M.K. Reser, G. Smith, and H. Insley, Eds., Symposium on nucleation and crystallization in glasses and melts, p. 47–54. The American Ceramic Society, Columbus, Ohio.

Carroll, M.R. and Holloway, J.R. (1994) Volatiles in magmas. In Mineralogical Society of America Reviews in Mineralogy, 30, 1–517.

Cashman, K.V. (1992) Groundmass crystallization of Mount St. Helens dacite, 1980-1986: a tool for interpreting shallow magmatic processes. Contributions to Mineralogy and Petrology, 109, 431–449.

Cashman, K.V., Hammer, J.E., and Rogers, J. (1996) Degassing-induced crystallization and the nature of pulsatory eruptions. Eos, 77, p. F819.

Cashman, K.V. and Marsh, B.D. (1988) Crystal size distribution (CSD) in rocks and the kinetics and dynamics of crystallization II: Makaopuhi lava lake. Contributions to Mineralogy and Petrology, 99, 292–305.

Christian, J.W. (1975) The Theory of Transformations in Metals and Alloys. Pergamon Press, Oxford.

Davis, K.M. (1994) The diffusion of water into silica glass at low temperatures, p. 370. Materials Engineering, Rennselaer Polytechnic Institute, New York.

Davis, M.J. (1996) Influence of water and thermal history on viscosity and nucleation kinetics of lithium disilicate melt, p. 159. Geology and Geophysics, Yale University, Connecticut.

Davis, M.J., Ihinger, P.D., and Lasaga, A.C. (1997) Influence of water on nucleation kinetics in silicate melt. Journal of Non-Crystalline Solids, 219, 62–69.

Fratello, V.J., Hays, J.F., and Turnbull, D. (1980) Dependence of growth rate of quartz in fused silica on pressure and impurity content. Journal of Applied Physics, 51, 4718–4728.

Gonzalez-Oliver, C.J.R., Johnson, P.S., and James, P.F. (1979) Influence of water content on the rates of crystal nucleation and growth in lithia-

silica and soda-lime-silica glasses. Journal of Material Science, 14, 1159–1169.

Holand, W., Frank, M., and Rheinberger, V. (1995) Surface crystallization of leucite in glasses. Journal of Non-Crystalline Solids, 180, 292–307.

Hurwitz, S. and Navon, O. (1994) Bubble nucleation in rhyolitic melts: Experiments at high pressure, temperature and water content. Earth and Planetary Sciences, 122, 267–280.

James, P.F. (1974) Kinetics of crystal nucleation in lithium silicate glasses. Physics and Chemistry of Glasses, 15, 95–105.

James, P.F. and Keown, S.R. (1974) Study of crystallization in lithium silicate glasses using high-voltage electron microscopy. Philosophical Magazine, 30, 789–802.

Kesler, S.E. and Weiblen, P.W. (1968) Distribution of elements in a spherulitic andesite. American Mineralogist, 53, 2025–2035.

Khoury, F. and Passaglia, E. (1976) The morphology of crystalline synthetic polymers. In N.B. Hannay, Ed., Crystalline and Noncrystalline Solids, p. 335–496. Plenum Press, New York.

Kirkpatrick, R.J., Klein, L., Uhlmann, D.R., and Hays, J.F. (1979) Rates and processes of crystal growth in the system anorthite-albite. Journal of Geophysical Research, 84, 3671–3676.

Klug, C. and Cashman, K.V. (1994) Vesiculation of May 18, 1980, Mount St. Helens magma. Geology, 22, 468–472.

Leko, V.K. and Komarova, L.A. (1975) Crystallization of quartz glasses in different gaseous media. Inorganic Materials, 11, 950–953.

Lofgren, G.E. (1971) Spherulitic textures in glassy and crystalline rocks. Journal of Geophysical Research, 76, 5635–5648.

———(1983) Effect of heterogeneous nucleation on basaltic textures: a dynamic crystallization study. Journal of Petrology, 24, 229–255.

Maleev, M.N. (1972) Diagnostic features of spherulites formed by splitting of a single-crystal nucleus. Growth mechanism of chalcedony. Tschermaks Mineralogische und Petrographische Mitteilungen, 18, 1–16.

Matusita, K. and Tashiro, M. (1973) Rate of homogeneous nucleation in alkali disilicate glasses. Journal of Non-Crystalline Solids, 11, 471–484.

Mishima, N., Ota, R., Wakasugi, T., and Fukunaga, J. (1996) Analysis of crystallization behavior in Li_2O $2SiO_2$ glass by DTA method based on a liquid model. Journal of Non-Crystalline Solids, 197, 19–24.

Narayan, K.L., Kelton, K.F., and Ray, C.S. (1996) Effect of Pt doping on nucleation and crystallization in Li_2O $2SiO_2$ glass: experimental measurements and computer modeling. Journal of Non-Crystalline Solids, 195, 148–157.

Philpotts, A.R. and Lewis, C.L. (1987) Pipe vesicles-An alternate model for their origin. Geology, 15, 971–974.

Planner, H.N. (1979) Chondrule thermal history implied from olivine compositional data, p. 150. Geology, University of New Mexico, Albuquerque.

Rosen, M.J. (1989) Surfactants and Interfacial Phenomena. Wiley, New York.

Schlesinger, M.E. and Lynch, D.C. (1989) Effect of VB and VIB oxides on nucleation parameters in lithium disilicate glass. Journal of Non-Crystalline Solids, 108, 237–248.

Schmelzer, J., Pascova, R., Moller, J., and Gutzow, I. (1993) Surface-induced devitrification of glasses: the influence of elastic strains. Journal of Non-Crystalline Solids, 162, 26–39.

Taylor, B.E., Eichelberger, J.C., and Westrich, H.R. (1983) Hydrogen isotopic evidence of rhyolitic magma degassing during shallow intrusion and eruption. Nature, 306, 541–545.

Wilcox, W.R. and Kuo, V.H.S. (1973) Gas bubble nucleation during crystallization. Journal of Crystal Growth, 19, 221–228.

Zanotto, E.D. and James, P.F. (1985) Experimental tests of the classical nucleation theory for glasses. Journal of Non-Crystalline Solids, 74, 373–394.